2021 43rd Annual International Conference of the
IEEE Engineering in Medicine & Biology Society (EMBC)
Oct 31 - Nov 4, 2021. Virtual Conference

Detection of Arcing and High Impedance with Electrical Weapons

Bryan D. Chiles, ASE, *Member IEEE*; Max H. Nerheim, MSEE, *Member IEEE*; Ryan C. Markle, BSEE, *Member IEEE*; Michael A. Brave, MS, JD, *Sr. Member IEEE*; Dorin Panescu, PhD, *Fellow IEEE*, and Mark W. Kroll, PhD, *Fellow IEEE*

Introduction: Conducted electrical weapons are primarily designed to stop subjects from endangering themselves or others by deploying 2, or more, probes to conduct current via the body to induce motor-nerve mediated muscle contractions, but probe impedance can vary significantly including open circuits from probes failing to complete or maintain a circuit.

Methods: We tested 10 units of the TASER® 7 model with a range of impedances and open circuit conditions. Pulse data (stored in the device's memory) were used to predict the load resistances and detect arcing conditions. Acoustical data (recorded externally) was evaluated on an exploratory basis as a secondary goal.

Results: The average error of predicted resistance, over the physiological load range of 400–1000 Ω, was 8%. Arcing conditions was predicted with an accuracy of 97%. An arcing condition increases the duration of the sound generation.

Conclusions: The TASER 7 electronic control device stored pulse-log data for charge and arc voltage yielded forensic analysis of the load resistance with reliable accuracy.

I. Introduction

The first conducted electrical weapon (CEW) to reliably induce involuntary muscle incapacitation and provide digital logs of basic activation data was the Advanced TASER® M26 (1999). The X26E model (2003) introduced shaped-pulse™ technology which cut the power consumption from ≈ 50 W to ≈ 12 W, further increased subject incapacitation performance, reduced the CEW's physical size by 2/3rd for easier carry, and stabilized the pulse rate at ≈ 19 Pulses Per Second (PPS), a significant improvement from the M26 technology where the pulse rate was dependent on battery type and charge level.

The 3-shot X3 (2009) introduced charge metering which utilized a feed-forward control method to keep the delivered charge constant and independent of arcing or load impedance, in prior technologies the charge delivery and thus subject incapacitation performance was highly dependent on whether the device was arcing (to make a connection) or had an ohmic connection. The X3 also introduced Trilogy Logs™, which include objective stored data for objective forensic analysis. The follow-on TASER X2 (2011, 2-shot) and X26P (2013, single shot) devices refined the X3 technology in physically smaller devices.

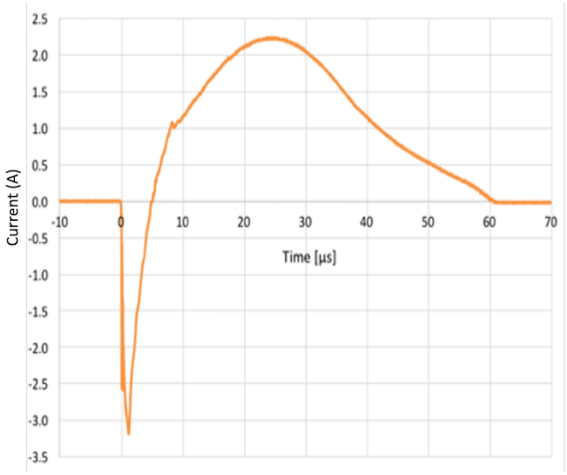

Figure 1. Typical T7 pulse with current (vertical axis) in amperes.

The T7 (2018) increased the pulse rate to 22 PPS, added wider-angle close-proximity cartridges (12° vs. 3.5° for the long-range cartridge), and added Adaptive Cross-Connect that increased the probability of effective electrical charge delivery in incidents including a missed, dislodged, or clothing disconnect probe deployment and various close probe-spread scenarios.

The innovations in the T7 are perhaps the most significant technology leap for probe-deploying CEWs since the introduction of the X26E in 2003. The prior multiple-cartridge versions of CEWs made by TASERTron, Carbon Arms, and the TASER X2 and X3 had very limited, if any, ability to channel current between probes from different cartridges. If all probes connected, the charge would be channeled mainly between each cartridge's probes with little or no current flowing between probes from different cartridges. However, if 1 of 4 probes missed, current could be

B. Chiles is Sr. Investigations Engineer at Axon Enterprise, Inc. (Axon) (e-mail: bchiles@axon.com).
M. Nerheim is Technical Fellow and Vice President of Research at Axon (e-mail: max@axon.com).
M. Brave is Manager/Member of LAAW International, LLC, an employee of Axon, and legal advisor to the Axon Scientific and Medical Advisory Board (SMAB) (e-mail: brave@laaw.com).
R. Markle is Sr. Electrical Engineer at Axon. (email: rmarkle@axon.com).
D. Panescu is Chief Technical Officer, Vice President R&D, HeartBeam, Inc. (e-mail: panescu_d@yahoo.com). Dr. Panescu is a paid consultant to Axon.
M. Kroll is Adj. Prof. of Biomedical Engineering at California Polytechnical Univ. (e-mail: mark@kroll.name). Member of Axon Corporate & Scientific Advisory Board.
All authors have served as consultants and expert witnesses for Axon, law enforcement, or in Coroners' Proceedings. Research supported by Axon.

channeled to a single probe. The T7 channels current equally well between any top to any bottom probe even if all 4 probes are connected, or if only one top and one bottom probe from either of the 2 cartridges is connected, increasing subject incapacitation performance in numerous field scenarios, especially if each cartridge has a narrow probe spread but there is a larger spread between each of the cartridge deployments. Probe spread is critical to successful incapacitation performance with a spread of ≈ 30 cm being required on the front of the body and 20 cm on the back due to the proximity to the largest extremity nerves.[1] Even though the spacing between each pair of probes is not sufficient, the output switching circuitry of the T7 allows a connection to be made between whichever probes will give the longest vector spread.

Generating the high-voltage output pulse of all CEWs, prior to the T7, utilized a single output transformer for each high voltage pulse. Each transformer had 2 fixed output leads connecting to 2 probes. A 1-cartridge device had a single output transformer, a 2-cartridge device had 2 transformers, and so on. Since only a single transformer was activated per pulse, and since it energized both cartridge probes, there was no capability to create an effective electrical "cross connect" pathway connecting a probe from a given cartridge to a probe on a different cartridge.

The T7 high-voltage output circuit utilizes 1 output transformer per probe for each of its' 2 cartridges with 2 probes each, for a total of 4 output transformers; 2 are configured as "positive" arc, and 2 as "negative" arc transformers. Each cartridge has a positive "top" probe and a negative "bottom" probe, connected to respective arc transformers. By activating a specific positive and a specific negative arc transformer, any combination of positive to negative probe combinations can be energized: from cartridge 1 top probe to bottom probe, from cartridge 2 top probe to bottom probe, from cartridge 1 top probe to cartridge 2 bottom probe, and from cartridge 2 top probe to cartridge 1 bottom probe.

The T7 also senses where the current is actually flowing, and determines the connection quality, based on stimulation voltage, charge delivered, and charge return path measurements. As a result, it determines which probes are connected to a target, and which are not. The device's output of up to 44 PPS is distributed among the 4 possible probe combinations according to connection quality with the best connections receiving a higher pulse rate, and the poorer connections less. As the measured connection quality is changing in real time, the pulse distribution is redistributed among the 4 probe-pair combinations in real time pulse-by pulse to increase subject incapacitation performance. This adaptive-pulse distribution strategy enabled by the "dedicated transformer per probe" technology, charge sensing, and current path sense circuits is called Adaptive Cross Connect (ACC™).

The ACC technology is a significant advance on prior technologies, providing increased subject incapacitation performance under a broader range of challenging circumstances. The high-voltage circuitry in the T7 device consists of a section (Figure 2) for charging the pulse capacitors, and another (Figure 3) for discharging the pulse capacitors and creating the output waveform. As shown in Figure 2 the capacitor charge circuit works as a flyback power supply. When transistors Q1 or Q2 are enabled by the Pulse Width Modulated (PWM) signal PWM_ARC and PWM_MUSCLE, energy is stored in transformers T1 and T2. When Q1 and Q2 are turned off, the stored energy is released through the secondary windings of transformer T1 and T2, through diodes D1, D2, and D3 into capacitors C1, C2, and C4. The PWM delivers pulses to Q1 and Q2 until the voltage at ARC_SNS, P_MUSCLE_SNS, and N_MUSCLE_SNS reach their desired values, corresponding to between 700–1000 V for C1, 1500- 3600 V for C2, and -1500–-3600 V for C4. The capacitor charge voltages are continuously adjusted to maintain consistent delivered charge regardless of delivery via arc or embedded probes.

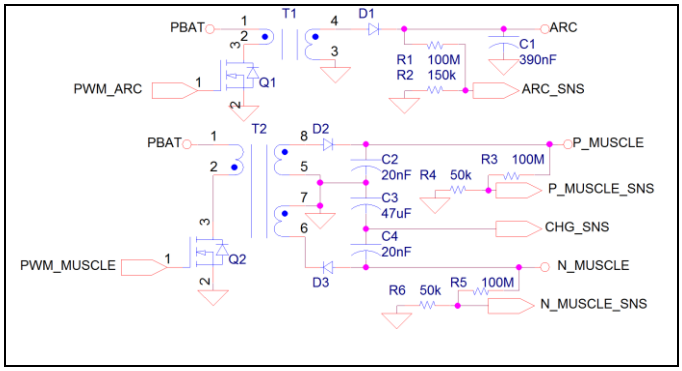

Figure 2. Capacitor Charge circuit

Each of 4 pulse discharge transformers, T3, T4, T5, and T6 in Figure 3 is able to create a positive or negative 25 kV high voltage pulse at their output terminals pin 1 to pin 2. A 50 kV potential difference overall is created between positive to negative arc voltages.

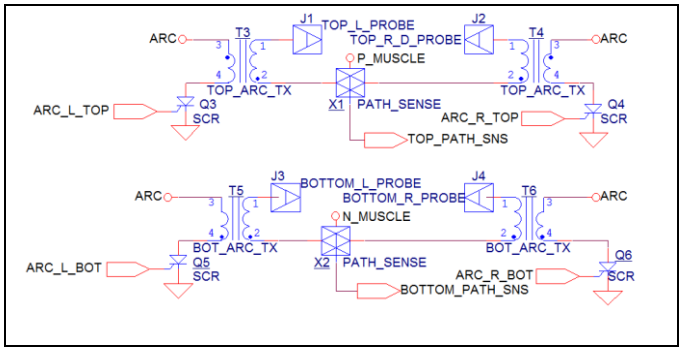

Figure 3. Capacitor Discharge circuit

The high voltage arc is created by turning on a top SCR and a lower SCR to conduct the energy stored in capacitor C1 through the arc transformer primary winding pins 3 to 4. The high turns ratio from primary to secondary windings on the pulse transformers converts the lower voltage stored on capacitor C1 to a positive and negative potential of up to ± 25 kV at the output terminals of the arc transformers. The high voltage is conducted thru the cartridge and isolated wires to the probes, and unless the darts are inserted into skin, the voltage can arc and create a 40 mm long path of ionized conductive air through thick clothing or other similar materials, allowing charge delivery without an ohmic connection. The arc and air ionization enables the current to

flow from the P_MUSCLE capacitor C2, through the path sense circuitry, through secondary pins 2 to 1 of the activated TOP_ARC_TX transformer T3 or T4, to left or right top probe, through a possible air gap, into a subject, to a bottom probe, through the activated BOT_ARC_TX transformer, through the bottom path sense circuit, and into the N_MUSCLE capacitor C4. This repeats itself up to 44 times per second. The arc capacitor C1 is typically discharged from 1000–0 V in ≈ 1 μs by passing the discharge current of up to ≈ 800 A through the 2 selected SCRs. The output voltage reaches 50 kV in ≈ 1.5 μs. Each output pulse has a duration of ≈ 45 μs.

Each discharge will charge up capacitor C3 with a charge equivalent to what was just delivered through the probes. The microprocessor will read this charge, discharge the capacitor to be ready for the next pulse, and based on the just-measured data, modify the next charge level for capacitors C1, C3, and C4 to target the desired output charge, which is 63 μC for T7. At 44 PPS the T7 can deliver up to 63 μC * 44 PPS = 2.8 mA. The T7 microprocessor will also read sensor outputs from the TOP_PATH_SENS and BOT_PATH_SNS circuits after each discharged to determine if the discharge current chose the path that was intended, or a different path. By comparing data from charge delivery, capacitor voltage charge levels, and path sense circuits, T7 efficiently and effectively determines probe connection quality and distributes varying pulse rates to different connected probe pairs to dynamically improve and maximize subject incapacitation performance.

The exemplar CEW pulse shown in Figure 1 used a 600 Ω load. By convention, the "main" phase is defined as being positive and delivers most of the charge.[2] The initial negative-phase makes an electric arc to bridge an air gap when there is no direct connection. CEWs are controlled by the ANSI (American National Standards Institute) CPLSO-17 (2017) standard.[3] The "raw charge" is the integrated value across the full duration of the pulse. Note that the raw charge is always *less* than that of the main phase since the arc phase contributes a *negative* charge, thus subtracting. Since the arc-phase has ≈ 5 μC, the main-phase charge equals the raw-charge plus 5 μC.

The primary goal of this study was to explore the T7 load limits where the charge metering feedback system can maintain the charge at the target level. The secondary goal was to evaluate the methodological reliability of the Pulse Log stored objective data to reasonably estimate the load resistance value and to diagnose open-circuit muzzle arcing.

II. Methods:

We tested 10 T7 units. We used non-inductive high-voltage resistor assemblies of 50, 200, 400, 600, 1k, 1.5k, 2.5k, 3.5k, 5k, 10 kΩ, a shorted output (nominal 0 Ω), and various open-circuits (to cause arcing across the CEW muzzle). A Stangenese "0.5–1.0 W" model high-frequency 0.5% accuracy current transformer was used to monitor the outputs to verify operation of the CEW.

The Pulse Log data were downloaded to provide the charge and the stimulation and arc voltages for each of the pulses in a single 5 s standard delivery cycle.

The Pulse-Log includes the pulse-by-pulse voltage stored on the arc and stimulation capacitors and the measured charge. The arc voltage is the voltage across the arc capacitors driving the primary of the output transformer. This voltage shows what level the capacitors needed to be in order to generate an output pulse. The stim voltage is the voltage across the stimulation capacitor which is dumped directly into the output connections in series with the transformer secondary and shows what level the capacitors needed to be in order to produce the electrical output charge measured.

The "Charge Metering" described above regulates the raw output charge to a target level of 63 μC. (Note that this implies a main-phase charge of ≈ 68 μC.) When the CEW trigger is first pulled, the arc and stimulation capacitors are charged to a nominal voltage. If the measured charge is significantly different than the target value, the charge-voltages of the arc and stim capacitors are adjusted up or down before the next pulse. The charge is measured on every pulse, and every next capacitor charge voltage is adjusted accordingly. For extreme load values, stability of the charge obtains in about 200–400 ms. If the load impedance is very high (> 1 kΩ), resulting in lower charge, the arc and stim voltages are increased up to the maximum voltage allowed for the capacitors, and the delivered charge will not increase further, unless the load impedance drops. If the load impedance drops and the charge increases *above* the target value, the CEW will lower the voltage on the arc and stim capacitors until the charge drops to the target value.

The capacitor charge voltages adjust downward initially for the 0 Ω load while adjusting upward for the 600 Ω and 5 kΩ loads. To allow for the charge-metering adjustments during our testing, the initial 1 second was ignored and only the last 4 seconds (≈ 88 pulses) were analyzed. These were averaged to produce a charge value and arc and stim voltages for each load and unit. The standard deviations of these values were also calculated over the 4 s period.

III. Results:

A. Resistance Modeling

JMP v14.0 was used for statistical analysis. For the resistance modeling, the samples of muzzle arcing were excluded. Attempts were made to predict the load resistance with an omnibus multiple-regression model, but this proved impractical. There is a sharp inflection point at 1 kΩ (load resistance) and 60 μC (delivered charge). We then fit the data with a 2-piece model bifurcated at Q = 60 μC.

For Q ≥ 60 μC the prediction model was:

$$R = 0.0001146\ V_{stim}^2 - 245 \quad (1)$$

Where V_{stim} is the arcing voltage (V) and Q is the charge (μC). Note that V_{arc}/Q would be an Ohm's law analog for the resistance, but the quadratic fit was better.

This overall model had $r^2 = 0.97$. The RMS prediction error was 70.1 Ω. The average error over the physiological load range of 400–1000 Ω was 8%.

For Q < 60 μC, an efficient model was:

$$R = 998314/Q - 16196 \quad (2)$$

This had $r^2 = 0.87$ with a RMS error of 1090 Ω. That error was dominated by the largest R values. The average error was 22%.

A more complex (4-factor) model was:

$$R = 1.725Q^2 - 1207938/Q - 100V_{stim}^2 + 6229\,\sigma(Q) - 25767$$

where σ is the standard deviation. The average error was 13%. The T7 model satisfied the ANSI raw charge minimum value of 40 µC for loads up to 5 kΩ. For physiological loads (400–1000 Ω) the average net charge reported by the pulse graphs was 62.4 ± 2.4 µC which closely matched the external recording of 62.9 ± 2.4 µC by digital oscilloscope recording. There was no violation of the ANSI upper limit of 125 µC.

The overall 2-piece model performance is shown in Figure 4. (Negative value predictions were set to 0 Ω.) Note that the simple (1-factor model) had more extreme prediction errors.

When the load resistance is > 1 kΩ, the circuitry runs open-loop and thus the variability of the charge, and hence of the resistance predictions, increase significantly. Consequently, predictive accuracy is reduced (± 13%). However, for the physiological loads, which are ≤ 1 kΩ, the predictive accuracy is quite good.

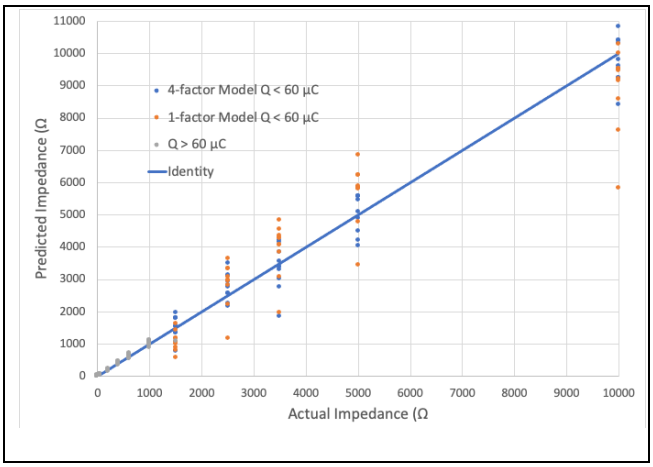

Figure 4. Predicted vs actual resistance.

B. Muzzle Arcing

With an open circuit — from a broken wire or dislodged probe — the CEW will arc across the muzzle and output a full normal charge (on average). In addition, the recorded parameters are consistent with typical load resistances and thus the above prediction models would give misleading load estimates. However, since every pulse requires ionization of the air and hence, each pulse is discharged into a different "load", the instability of the arc increases the standard deviation of the charge as seen in Figure 5. and this can be reliably used.

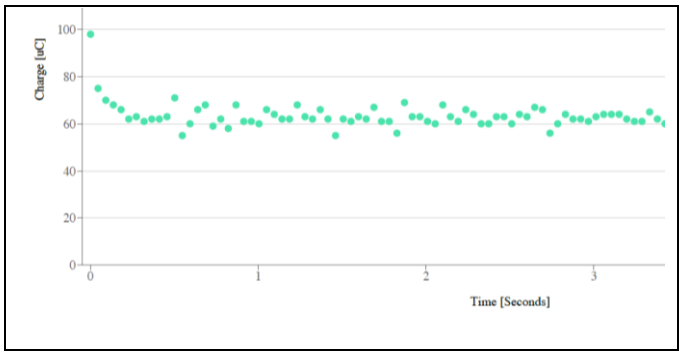

Figure 5. Delivered charge during arcing conditions.

There are 3 different open-circuit conditions: (1) Probes deployed with no connection, (2) probes deployed but arcing, and (3) arcing across the distal end of the cartridge muzzle. With probes deployed but no wire separation, the capacitive and inductive loads of the wires prevented the high-voltage formation of an arc and there is no charge delivered. The delivered charge is typically recorded as 1 or 2 µC which differentiates easily from the other arcing conditions.

We ignored non-physiological loads (< 200 Ω) and charges < 60 µC. With a simple cutoff using σ (Q) ≥ 1.8 µC, we correctly identified all 20/20 arcing tests and had only 3/90 false positives where physiological loads were incorrectly identified as arcing. Due to the small residual data set we are unable to provide sufficient data for a meaningful discriminant function calculation using a quadratic (differing covariance) model to differentiate open circuit arcing from a resistive load.

Arcing can also be potentially detected by acoustical analysis from recorded media-audio which is increasingly important with the advent of body worn cameras on law-enforcement officers. We recorded the sound of the CEW discharge with a Tascam model DR-07X digital recorder located 1 m away in an anechoic chamber, comparing the discharge in open air to discharge into a resistive load. The audio files were analyzed using Sonic Visualizer version 4.2.

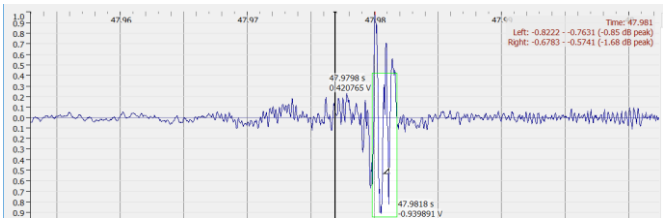

Figure 6. Time domain sound pressure level with a resistive load.

With a resistive load there is some sound generated due to the operation of the high-voltage circuitry, but this persisted for only about 2 ms as seen in Figure 6. With arcing significantly more sound is generated due to the air breakdown as seen in Figure 7. This is consistent with present understanding of the crackling sound emitted from an electrical arc.[4-6]

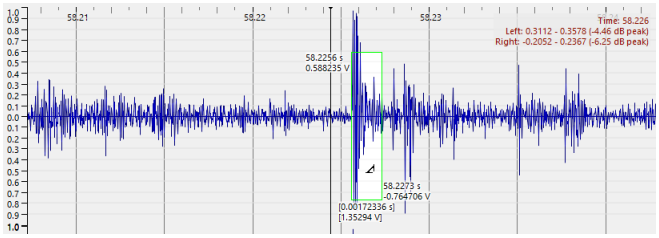

Figure 7. Time domain sound pressure level with arcing.

IV. Discussion

Human electronic control has gained widespread acceptance as an intermediate-force option. Presentation 2/3.[7, 8] Subject injuries, requiring medical attention, are reduced by 80%.[9] The short-duration pulses stimulate Type A-α motor neurons, to control skeletal muscle contraction, but with minimal risk of stimulating myocardium. This typically leads to a loss of regional muscle control and can result in a fall to the ground to end an immediate threat or flight risk.[1, 10, 11]

However, there are many cases where the electronic control fails, and this can result in a fatality.[12, 13] Thus, it is very important to be able to diagnose the source of the problem and understand the contribution of the body impedance and lead failures.

V. Limitations

The Pulse Logs can provide reliable objective evidence of a charge delivered into a load. They do not provide any evidence of the nature of the load (human, animal, water, or other). The Pulse Logs give no definitive indication of incapacitation performance as that is affected by a myriad of factors including probe spread and locations and other factors on the body.[1]

VI. Conclusion

For physiological loads (400–1000 Ω) the average net charge reported by the T7 pulse graphs was 62.4 ± 2.4 µC which closely matched the external recording of 62.9 ± 2.4 µC. The presence of arcing can be diagnosed using the variability of the charge and stimulation voltage as well as the duration of the high sound-pressure level from the arcing sound.

References

[1] J. Ho, D. Dawes, J. Miner, S. Kunz, R. Nelson, and J. Sweeney, "Conducted electrical weapon incapacitation during a goal-directed task as a function of probe spread," *Forensic Sci Med Pathol,* vol. 8, no. 4, pp. 358-66, Dec 2012, doi: 10.1007/s12024-012-9346-x.

[2] A. Adler, D. Dawson, and I. Sinclair, "Test Procedure for Conducted Energy Weapons v2.0," p. 45, 2017. [Online]. Available: https://curve.carleton.ca/system/files/faculty_staff_research_publication/c38e4395-6454-4ab7-9d45-b8f9796d7b65/fac_staff_res_pub_pdf/8a2e7c3e11acea1c5040545b351b4c89/cewtest-procedure-2017-ver20.pdf.

[3] *Electrical characteristics of ECD's and CEW's.*, ANSI, Bristol, UK, 2017. [Online]. Available: https://estandards.net/product/ansi-cplso-17/

[4] R. Robson and B. Paranjape, "Acoustoelectric effects in a gaseous medium," *Physical Review A,* vol. 45, no. 12, pp. 8972-8974, 1992.

[5] P. Bequin and P. Herzog, "Model of acoustic sources related to negative point-to-plane discharges in ambiant air," *Acta Acustica,* vol. 83, pp. 359-366, 1997.

[6] P. Bayle, J. Vacquie, and M. Bailey, "Cathode region of a transitory discharge in CO2. I. Theory of the cathode region," (in Eng), *Phys Rev A,* vol. 34, no. 1, pp. 360-371, Jul 1986.

[7] F. V. Ferdik, R. J. Kaminski, M. D. Cooney, and E. L. Sevigny, "The Influence of Agency Policies on Conducted Energy Device Use and Police Use of Lethal Force," *Police Quarterly,* p. 1098611114548098, 2014.

[8] M. Kroll, M. Brave, H. Pratt, K. Witte, S. Kunz, and R. Luceri, "Benefits, Risks, and Myths of TASER® Handheld Electrical Weapons," *Human Factors and Mechanical Engineering for Defense and Safety,* vol. 3, no. 1, p. 7, 2019.

[9] B. Taylor and D. J. Woods, "Injuries to officers and suspects in police use-of-force cases: A quasi-experimental evaluation," *Police Quarterly,* vol. 13, no. 3, pp. 260-289, 2010.

[10] J. C. Criscione and M. W. Kroll, "Incapacitation recovery times from a conductive electrical weapon exposure," *Forensic Sci Med Pathol,* vol. 10, no. 2, pp. 203-7, Jun 2014, doi: 10.1007/s12024-014-9551-x.

[11] J. Ho *et al.*, "A comparative study of conducted electrical weapon incapacitation during a goal-directed task," *Forensic Sci Med Pathol,* vol. 16, no. 4, pp. 613-621, Dec 2020, doi: 10.1007/s12024-020-00284-7.

[12] M. W. Kroll and M. A. Brave, "Defending Non-Firearm Arrest-Related Death Incidents," *International Municipal Lawyers Association,* p. https://www.researchgate.net/publication/342064787, 2020.

[13] H. E. Williams, D. Reinhard, and T. B. Oriola, "Fatal officer involved shootings following the use of TASER conducted energy weapons," *The Police Journal,* p. 0032258X211030322, 2021.